Clim Dyn (2009) 32:19–33
DOI 10.1007/s00382-008-0366-x

# Intense coastal rainfall in the Netherlands in response to high sea surface temperatures: analysis of the event of August 2006 from the perspective of a changing climate

**G. Lenderink · E. van Meijgaard · F. Selten**

Received: 19 September 2007 / Accepted: 4 January 2008 / Published online: 30 January 2008


**Abstract** August 2006 was an exceptionally wet month in the Netherlands, in particular near the coast where rainfall amounts exceeded 300% of the climatological mean. August 2006 was preceded by an extremely warm July with a monthly mean temperature of almost 1°C higher than recorded in any other summer month in the period 1901–2006. This had resulted in very high sea surface temperatures (SSTs) in the North Sea at the end of July. In this paper the contribution of high SSTs to the high rainfall amounts is investigated. In the first part of this study, this is done by analyzing short-term integrations with a regional climate model (RACMO2) operated at 6 km resolution, which are different in the prescribed values of the SSTs. In the second part of the paper the influence of SSTs on rainfall is analyzed statistically on the basis of daily observations in the Netherlands during the period 1958–2006. The results from both the statistical analysis as well as the model integrations show a significant influence of SSTs on precipitation. This influence is particularly strong in the coastal area, that is, less than 30–50 km from the coastline. With favorable atmospheric flow conditions, the analyzed dependency is about +15% increase per degree temperature rise, thereby exceeding the Clausius–Clapeyron relation—which is often used as a temperature related constraint on changes in extreme precipitation—by approximately a factor of two. It is shown that the coastal area has consistently become wetter compared to the inland area since the 1950s. This finding is in agreement with the rather strong observed trend in SST over the same period and the dependencies of rainfall on SST reported in this study.

G. Lenderink (✉) · E. van Meijgaard · F. Selten
Climate Research Department, KNMI,
PO Box 201, 3730 AE De Bilt, The Netherlands
e-mail: lenderin@knmi.nl

## 1 Introduction

It is generally anticipated that the future climate of the central, western part of Europe (Germany, France, Belgium, The Netherlands) in summer will be dryer. The majority of the 4AR IPCC Global Climate Model (GCM) runs predict on average dryer conditions in summer (Christensen et al. 2007b). Major processes that are expected to establish or enhance the dry summer climate are circulation changes with more anti-cyclonic flows over western Europe (Van Ulden and Van Oldenborgh 2006) and large scale drying of the soil (Seneviratne et al. 2002; Vidale et al. 2007). In general terms, GCMs predict a decrease in summer precipitation in the southern part of Europe and an increase in the Northern part. The transition region between the increase in the north and the decrease in the south is projected to be relatively close to the Netherlands. Therefore, the change in precipitation is relatively uncertain. Not all 4AR GCMs agree on the decrease of mean precipitation, but a few simulations actually predict an increase (e.g., Van Ulden and Van Oldenborgh 2006).

It is also generally thought that, notwithstanding the decrease in mean summer precipitation as climate changes, the daily extremes will increase due to the larger moisture-holding capacity of air in a warmer climate. Numerous studies reported increases in daily precipitation extremes in global and regional climate models (RCMs) (e.g., Pall et al. 2007; Christensen and Christensen 2003; Räisänen et al. 2004; Frei et al. 2006). In agreement, observed daily precipitation extremes appear to have increased during the last

century (e.g., Groisman et al. 2005). Evidence from GCMs suggests that changes in the extremes are relatively well constrained by the Clausius–Clapeyron (CC) relation (Allen and Ingram 2002; Pall et al. 2007). The CC relation (hereafter CC relation), which determines the water vapor content of the atmosphere in saturated conditions as a function of temperature and pressure, gives an increase of approximately +7% per degree temperature change. Rainfall intensities in convective showers may increase even stronger than the CC relation. Latent heat release associated with precipitation formation may intensify the convective motions, thus leading to a positive feedback (Trenberth et al. 2003). Although the increase of the extremes appears to follow the CC relation rather closely, the global mean precipitation increases only at a rate of 1–3% per degree in GCMs. This sub-CC scaling can be explained by constraints due to the energy budget at the surface (Held and Soden 2006) or in the atmosphere (Allen and Ingram 2002).

In line with the above considerations, a new set of climate scenarios for the Netherlands, the KNMI'06 scenarios, was released in spring 2006 by the Royal Netherlands Meteorological Institute (KNMI) (Van den Hurk et al. 2006). Lenderink et al. (2007) describe how these scenarios were constructed based on results of GCMs (Van Ulden and Van Oldenborgh 2006) combined with results of RCM integrations from the PRUDENCE project (Christensen et al. 2007a). For summer two types of scenarios were issued: one type characterized by significantly dryer summer conditions where circulation changes and soil drying limit precipitation formation; the other characterized by a small increase in summer precipitation and no significant limitations due to circulation changes and soil drying. For the mean precipitation change between 1990 and 2050, the "dry" scenarios project a change between −10 and −20%, and the "wet" scenarios between +3 and +6%. Daily precipitation extremes are projected to increase by +6 to +12% in the dry scenarios and +12 to + 25% in the wet scenarios.

The summer following the release of the KNMI'06 scenarios was exceptional in a climatological sense. July 2006 was extremely warm and dry in the Netherlands. With a monthly average temperature of 22.3°C recorded at De Bilt (location in Fig. 6), this month was about 1°C warmer than recorded in any other summer month in the period 1901–2006. During the last 2 days of July a change in weather regime took place whereby the very warm anticyclonic atmospheric circulation, that characterized most of July, was replaced by a cold cyclonic circulation. This northwesterly circulation (see Fig. 1) persisted during the whole month of August and gave rise to extreme precipitation in the Netherlands. In particular, the local precipitation amounts in the coastal zone less than 50 km from the coastline were exceptionally high. At some coastal stations precipitation totals were recorded up to five times the climatological average of August.

The events in the summer of 2006 prompted new questions concerning to influence of North Sea temperatures on precipitation in the Netherlands. At the end of July the North Sea was very warm, in particular in the coastal zones with temperature anomalies of 3–5°C compared to the ERA40 (Uppala et al. 2005) derived climatology for the period 1961–1990 (see also Sect. 3). By further destabilizing the atmosphere and enhancing surface evaporation, the high sea surface temperature (SST) is likely to have contributed significantly to the extreme precipitation in August. This hypothesis is further investigated in this study. It is studied how the influence of the SST extends inland. Further, it is investigated how this dependency on SST relates to the above mentioned CC scaling, and how this depends on the circulation.

There is an abundant amount of scientific papers about the influence of SSTs on the climate system, and in particular on precipitation, for example ranging from impacts on the intensity of tropical cyclones, impacts on the tropical and extra-tropical circulation, and impacts on the intensity of the Monsoon (see e.g., Webster et al. 2005; Messager et al. 2004). In the European region (including North Africa) some studies showed clear impacts of SST in the Mediterranean Sea and Baltic Sea on precipitation (Rowell 2003; Kjellström and Ruosteenoja 2007). Benestad and Melsom (2002) show a link between autumn precipitation in southern Norway and Atlantic SSTs. The spatial scales involved in these studies are, however, larger than the ones involved here. We focus on a typical scale ranging from ten to several hundreds of kilometers. A recent study in California shows considerable impacts of coastal SSTs on coastal precipitation on these scales (Persson et al. 2005). Several studies also showed impacts of Mediterranean SSTs on the intensity of mesoscale convective events (e.g., Lebeaupin et al. 2006, and references herein).

Given that, for the moment, we accept the influence of SST on precipitation, questions about the validity of the RCMs on which we based the KNMI'06 scenarios can be posed. These RCM integrations were performed during the years 2001–2004 in the PRUDENCE project (Christensen et al. 2007a) and did not include a model for the North Sea. Instead North Sea temperatures were prescribed from the driving GCM, which obviously lacks the resolution to resolve the North Sea. The North Sea is a shallow coastal sea (20–200 m deep) and therefore adapts, in comparison to the Atlantic ocean, relatively fast to changing atmospheric conditions. We note, however, that the Baltic Sea was included in some of the PRUDENCE RCMs, and that the inclusion made a major impact on precipitation in the RCM simulations (Kjellström et al. 2005; Kjellström and

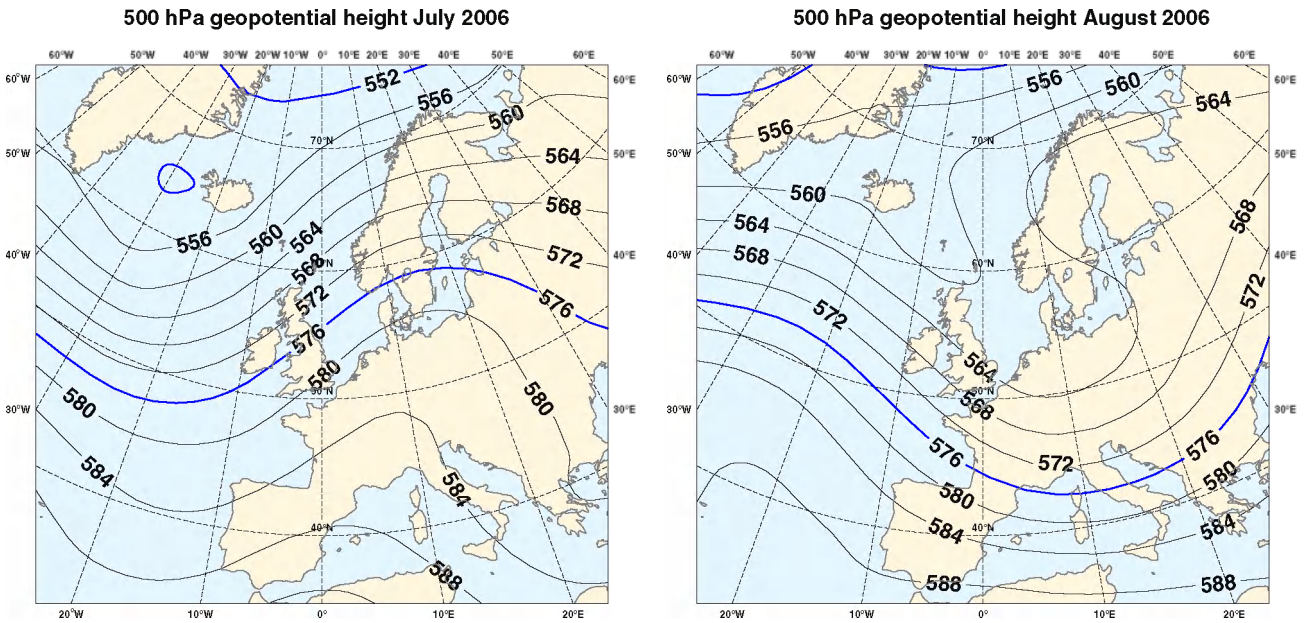


**Fig. 1** Synoptic situation during July (*left*) and August 2006 (*right*). Shown is the 500 hPa height obtained from the operational ECMWF analyses

Ruosteenoja 2007; Semmler and Jacob 2004). Also, Somot et al. (2007) discuss a long climate integration with a RCM coupled to an ocean model of the Mediterranean Sea. Despite these developments, coupled regional atmosphere–ocean climate models are not commonplace. For example, a recent large set of RCM runs performed in the EU-funded ENSEMBLES project (Hewitt and Griggs 2004) still uses prescribed SSTs as provided by the global models.

To establish whether the North Sea may significantly influence the precipitation climate in the Netherlands, and whether this could also impact climate change in the Netherlands, we will first present some trends in precipitation and SST of the North Sea over the last 55 years in Sect. 2. Motivated by these trends and by the event of August 2006, we continue to investigate the causal relation between SST and precipitation in a set of simulations with a RCM (Sect. 3) and by performing a statistical analysis using observations during the period 1958–2006 (Sect. 4). The paper concludes with a discussion of the results in a wider context and a short summary (Sects. 5, 6).

## 2 Observed trends in precipitation and SST

### 2.1 Precipitation measurements

Precipitation observations of approximately 320 stations in the Netherlands are used (see left-hand panel of Fig. 5 for the location of these stations). These observations are collected by KNMI and are available for the period 1951–2006. Before 1951 data of only a small number of stations is digitally available. Also, the height at which the measurements were taken was changed during the late 1940s with a significant impact on the measurements. Since 1951 the measurement method has not been changed significantly.

For the precipitation trends presented in this section and the statistical analysis in Sect. 4, spatial averages were computed for two regions: a coastal region with a border at 30 km from the coastline, and a remaining land region extending further inland (these regions can be found in Fig. 6 to be discussed below). As a relatively large fraction of the Netherlands is located close to the coast this separation gives roughly 150 stations in each region. The mean in the plots denotes the average of all stations in The Netherlands.

From the 320 stations, 238 stations have an almost continuous data record (data availability more than 98%) during the period 1951–2006, but only 149 stations have full data availability. In this paper we show the result using all stations available, since our main aim is to have the best possible representation of the area averaged precipitation. Results using the selection of 238 stations, however, are almost identical to the results presented in this paper, even for the trends computed in this section. Therefore, the impact of the data inhomogeneity appears minor.

### 2.2 Trends

Figure 2 shows the trend of the North Sea temperature during the period 1951–2006 estimated by linear

regression, together with the trend in global mean temperature and the temperature recorded at De Bilt (The Netherlands). For the SST we used the HadSST2 data set (Rayner et al. 2006) (average of the points at 2.5°E, 52.5°N and 2.5°E, 57.5°N). Despite the fact that this is a very coarse resolution data set, it has the advantage that it is corrected for spurious trends induced by changes in measurements conditions in time. In Sect. 4 daily time series of SST derived from the ERA40 re-analysis (Uppala et al. 2005), supplemented from 2003 until 2006 with the operational ECMWF analysis, are discussed. For comparison, we also show here the trend in SST derived from this time series for the period 1958–2006.

In summer, both SST data sets show that the temperatures in the North Sea do not follow the global trend, but rise faster. The trend in (late) summer is 1.2–1.5°C over the period considered, exceeding the trend in the global mean temperature by approximately a factor of two. In winter the two SST data sets disagree; the HadSST2 temperature rises faster than the global mean temperature, but the ERA40 derived temperature rises slower. Since our main focus is on summer precipitation, we did not further investigate this discrepancy. We note, however, that most of the discrepancy results from the early period before 1965.

The difference between the coastal precipitation and the inland precipitation displays a typical yearly cycle, with relatively dry conditions in the coastal zone during late spring and relatively wet conditions during autumn. The climatology of the precipitation difference over the period 1951–2006 as well as its trend over the same period is shown in the right-hand panel of Fig. 2. Uncertainty estimates of the regression coefficient are computed from the bootstrap using 200 samples drawn with replacement. In Fig. 2, the 10th and 90th percentiles of the regression coefficients obtained by the 200 bootstrap samples are plotted. The same procedure is used throughout this paper to estimate uncertainty. The trend in the precipitation difference between the coast and inland is considerable; apart from the spring months, the coastal zone is becoming wetter compared to the inland zone. The trend is largest in summer with an increase of 7–10 mm month$^{-1}$ over 55 years. Compared to the climatological average precipitation of approximately 70–75 mm month$^{-1}$ in summer these changes are considerable.

The difference between coastal and inland precipitation is a rather robust quantity showing the potential influence of the SST change. Trends in the precipitation difference do not strongly depend on the period that is analyzed. This is not the case for the total precipitation amounts in the coastal and inland zone separately. Figure 3 shows the 20-year moving average of the precipitation time series for late summer (JAS) for the period 1951–2006. Clearly the 1950s and 1960s were relatively wet, whereas the 1970s and 1990s were relatively dry. The period starting in the 1990s until present is again relatively wet. The trend in total precipitation amounts is strongly influenced by trends in the atmospheric circulation. Results of a regression model similar to that in Sect. 4, using different components of the geostrophic wind, showed that most of these temporal changes can be explained by circulation changes

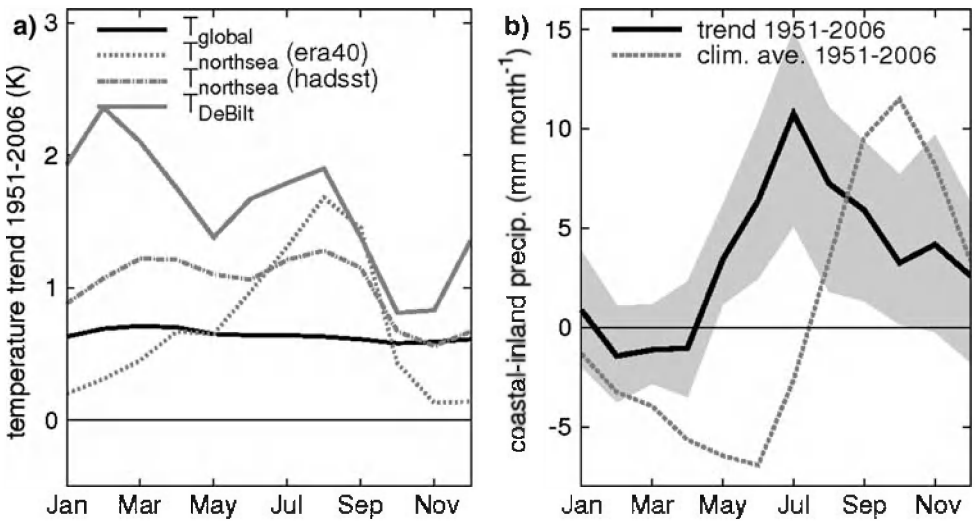


**Fig. 2** **a** Temperature trends in the period 1951–2006. Shown is the trend in global mean near surface temperature ($T_{GL}$), the temperature at De Bilt, the sea surface temperature (*SST*) in the North Sea derived from ERA40 (only 1958–2006 period) and derived from HadSST. **b** Precipitation difference between the coastal zone and the inland zone as a function of month. Shown is the climatology over the period 1951–2006 (*dashed line*) and the trend over this period (change in mm month$^{-1}$ per 55 year) (*thick solid line*, with the gray band indicating the 10–90% uncertainty range). Both plots are based on overlapping 3-month periods, e.g., Jul refers to the average of June, July, and August

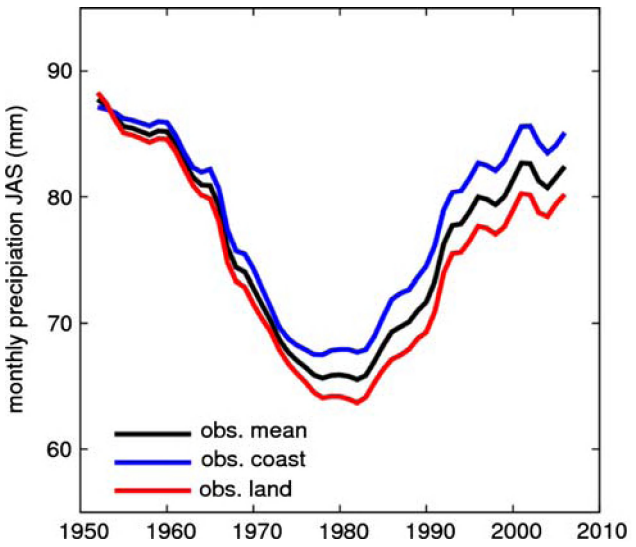


**Fig. 3** Time series of the 20-year moving average (smoothed with a 1-2-1 filter to remove high frequency noise) of mean, coastal and inland precipitation for late summer (July, August, September) in the Netherlands

(results not discussed in detail). We note that the atmospheric circulation displays a significant natural variability on a decadal time scale. Thus, atmospheric circulation changes are not necessarily related to global warming, although $CO_2$ induced climate change may cause shifts in circulation patterns (e.g., Yin 2005). In the 1950s precipitation amounts in the coastal and inland zone are approximately equal, but in the course of time the coastal zone is getting progressively wetter compared to the inland zone, consistent with Fig. 2. The estimation of a trend from the precipitation time series is extremely sensitive to the choice of the analysis period, and is not robust.

## 3 The case of August 2006

### 3.1 Experimental setup

Simulations with the KNMI regional atmospheric climate model RACMO2 are performed to assess the influence of SST in the North Sea on precipitation in the Netherlands. RACMO2 is a high resolution RCM based on hydrostatic dynamics originating from HIRLAM and physics of the European Centre of Medium Range Weather Forecast (ECMWF) (Lenderink et al. 2003). For this experiment a domain is chosen of approximately $1{,}000 \times 1{,}000$ km$^2$ (see Fig. 4) and a horizontal resolution of $6 \times 6$ km$^2$. The model uses 40 vertical levels. Lateral boundaries are given by the operational ECMWF analyses, updated each 6-h and using linear interpolation in time. The ECMWF analyses have a horizontal resolution of 1.5° and 91 levels vertically

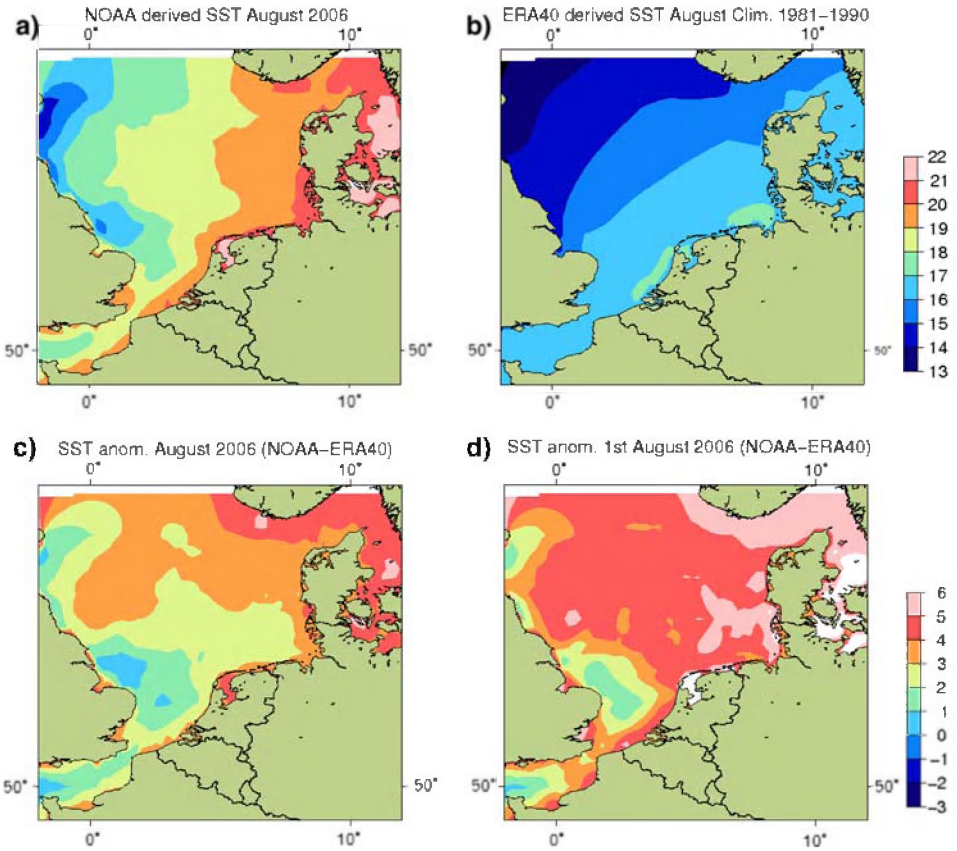


**Fig. 4** **a** Observed SSTs inferred from NOAA satellite measurements for August 2006, **b** ERA40 derived climatological SST for the period 1981–1990, **c** anomaly August 2006 NOAA SST compared to the ERA40 1981–1990 climatology, and **d** anomaly at 1 August 2006

**Table 1** Overview of the experiments with RACMO2

| Experiment | Derived from |
|---|---|
| NOAA | Observed SST derived from NOAA measurements |
| NOAAM2 | Observed SST like NOAA, but with 2°C subtracted |
| CL61-70 | ERA40 derived SST, average 1961–1970 period |
| CL71-80 | ERA40 derived SST, average 1971–1980 period |
| CL81-90 | ERA40 derived SST, average 1981–1990 period |
| CL90-00 | ERA40 derived SST, average 1991–2000 period |

(ECMWF uses a much larger number of levels in the stratosphere compared to RACMO2).

RACMO2 is operated in a hindcast mode; that is, consecutive model runs are started each day at 12 UTC from the ECMWF analysis. Each model integration is 36-h long, and the period from 12 to 36 h (0–24 UTC) is analyzed. This hindcast mode enforces the simulated atmospheric circulation to be very close to the observed circulation, which facilitates a comparison with observations on a daily level. Soil moisture was obtained from the ECMWF analysis, and was re-initialized each 36-h model integration. The soil moisture re-initialization prevents feedbacks through soil moisture, and therefore isolates the direct effect of SST on precipitation. Two additional experiments (for NOAA and CL81-90 SSTs; see Table 1) were performed in which each 36-h hindcast took the soil-moisture fields from the previous hindcast, thereby allowing a freely evolving soil moisture field in time. Results of these experiments (not discussed further) were almost identical to the results presented here, showing that soil-moisture feedbacks are small for this case. Finally, two climate integrations were performed, starting in June 2006 and running continuously until the end of August using the same ECMWF boundaries. Results of these experiments (again for NOAA and CL81-90 SSTs; see Table 1) were very close to those obtained in the hindcast mode on a monthly aggregated level, although on a daily level some substantial differences occurred. Therefore, for the measures presented in this paper the differences due to these modifications in the modeling setup are small compared to the influence of SST changes.

A set of model runs with different SSTs is performed as summarized in Table 1. The reference run (denoted by NOAA) uses the "observed" SST field derived from NOAA satellite measurements during August 2006 (see Fig. 4a). The SST is derived from weekly composites of the NOAA measurements at a $1 \times 1$ km$^2$ resolution, aggregated to the regional model grid and interpolated linearly in time assuming piecewise linear behavior in between. In addition to this run, several model runs with lower SSTs are performed. Ideally, a run with a high resolution climatological SST would provide a good background simulation, but accurate observations from the past to derive such a field are not available. Therefore, we relied on SSTs from the ERA40 reanalysis, which have a coarser resolution of typically 1°–2° (see Fig. 4b). Four runs with different 10-year climatologies (e.g., CL61-70 uses the ERA40 climatology of the period 1961–1970 for August) are performed. We note that the ERA40 climatologies of the 1960s (CL61-70), the 1970s (CL71-80), and the 1980s (CL81-90) are rather similar, with typical differences of only 0.5°C. All these SST climatologies lack the sharp gradients near the coast that were present in August 2006. Part of this gradient may be caused by the warm period preceding August 2006, but owing to the lack of a sufficiently long record of SST observations it is not possible to assess this effect precisely. We therefore supplemented the CL runs with one run (NOAAM2) in which the gradient near the coast is retained by subtracting 2°C from the NOAA observed SST for August 2006.

### 3.2 Results RCM simulations

The observed precipitation sum in August 2006 is shown in Fig. 5. Near the coast and Lake Yssel (located in the northwest of The Netherlands; see Fig. 6) the average precipitation sum is 210 mm, with maxima of near 300 mm at a few locations. Inland precipitation amounts are 150–180 mm on average. The climatological average (1971–2000) for August is 62 mm in the coastal area and 60 mm inland.

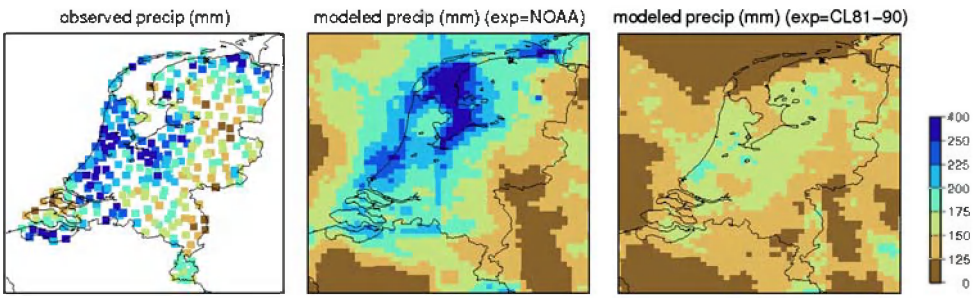


**Fig. 5** Observed precipitation amount (*left*), and modeled precipitation amount in experiments NOAA (*middle*) and CL81-90 (*right panel*) in August 2006 (mm)

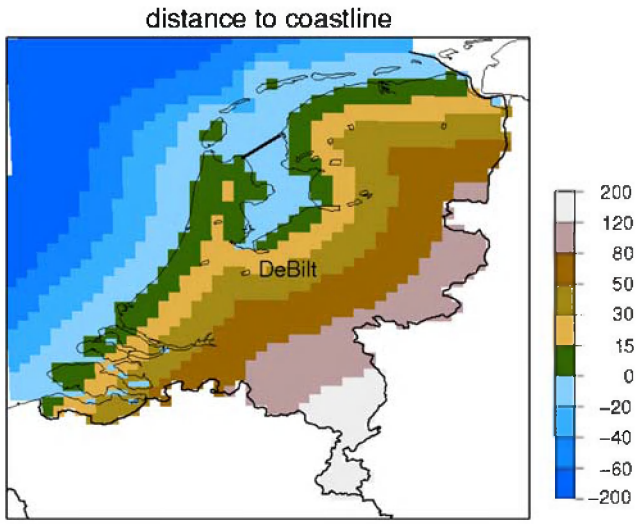


**Fig. 6** Division in zones based on the distance to the coastline. The big "lake" (separated by a dike) in the northwestern part is lake Yssel. Lake Yssel is included in the coastline

The simulated precipitation amounts for the experiments NOAA and CL81-90 are shown in Fig. 5b,c respectively. In the run with observed SST (NOAA) the regional model reproduces the high precipitation amounts in the coastal zone, and the lower amounts further inland. Despite the general correspondence, the maxima in precipitation do not always agree well with the observations, in particular near Lake Yssel where the model appears to produce unrealistically high precipitation amounts. Inspection of accumulated rainfall inferred from rain radar measurements did not show signs of the high amounts over Lake Yssel. It seems that the regional model reacts too quickly to the SST, therefore producing too much rain over sea and too little over land. The sensitivity experiment using the ERA40 derived SST 1981–1990 climatology (CL81-90) does not show the intensification of rainfall in the coastal area. The amounts further inland, however, are comparable to the reference experiment (NOAA). Results of the other sensitivity experiments are similar to CL81-90 with (very) weak coastal intensification of the rainfall.

To further quantify coastal effects, we analyzed rainfall as a function of distance to the coastline. For this purpose, different zones were defined based on the distance to the coastline (the coastline includes Lake Yssel). These different zones are shown for the model grid points in Fig. 6.

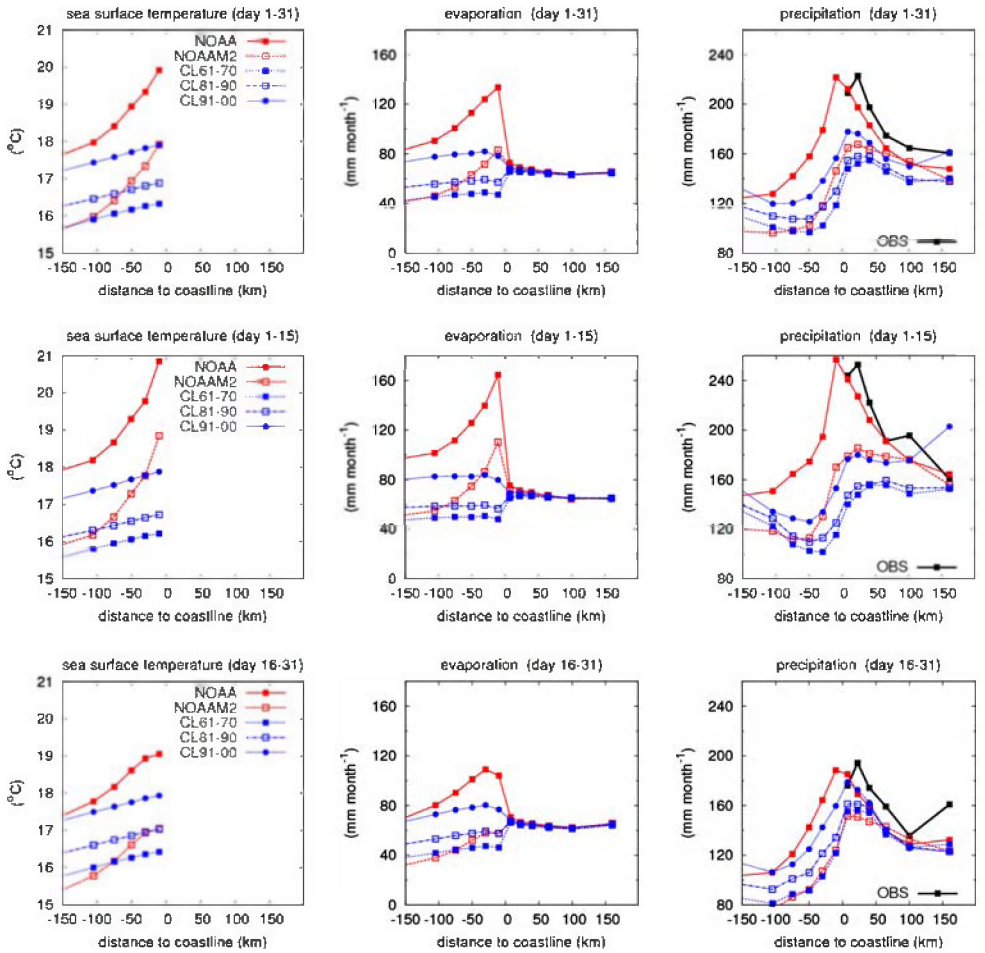


**Fig. 7** Sea surface temperature in °C (*left*), evaporation in mm month$^{-1}$ (*middle*) and precipitation in mm month$^{-1}$ (*right-hand panels*) as a function of distance to the coastline. The *upper panels* are based on the full month, the *middle* and the *lower panels* on the first half (days 1–15) and second half (days 16–31) of the month, respectively

Sea surface temperatures, evaporation rates and rainfall amounts are plotted in Fig. 7 as averages over the different zones. Monthly averages (upper) and also the averages corresponding to the first (middle) and the second half of the month (lower panel) are plotted (the latter amounts are converted to amounts equivalent to a month in order to facilitate the comparison). SST gradients near the coast in the CL runs are small due to the coarse resolution of the underlying ERA40 data. There is a large trend in time with the 1991–2000 period being approximately 1.5°C warmer than the 1961–1970 period. In response to the high SSTs in the coastal zone evaporation rates increase in the NOAA experiment from 80 mm month$^{-1}$ far away from the coast to 130 mm month$^{-1}$ near the coast. Evaporation rates in the sensitivity experiments near the coast are lower by 50–80 mm month$^{-1}$. Over land, evaporation rates in all experiments are comparable. An explanation could be the fact that the evolution of soil moisture was effectively prescribed by the soil moisture re-initialization. But, in two additional experiments with freely evolving soil moisture (for NOAA and CL81-90 SSTs) also very similar evaporation rates (differences less than 5 mm month$^{-1}$ with standard model setup) above land were found. Thus, soil moisture does not play a crucial role here.

Precipitation amounts over land in the NOAA experiment follow the observed precipitation rather closely, but there is spatial shift relative to the observations of approximately 20 km (shifted towards the sea) and the precipitation amounts are slightly lower. In all sensitivity experiments lower precipitation amounts in the coastal zone are simulated ranging from 30 to 60 mm month$^{-1}$. Further inland, the differences with NOAA are less than 20 mm month$^{-1}$. The middle and lower panels show that the sensitivity to the SST is concentrated in the first half of the month. We also note that the initially very warm seawater near the coast rapidly cooled in the course of the month (see Fig. 4d).

In the RACMO2 simulations there is a strong relation between the high SSTs and the enhanced evaporation over sea. A 1° higher temperature causes an additional evaporation of approximately 20 mm month$^{-1}$ (Fig. 8), which approximately corresponds to a 20% increase per degree. The relation between enhanced evaporation over sea and precipitation over land is weaker, but still apparent. The difference in evaporation over sea between the experiments is comparable to the difference in precipitation amounts in the coastal zone. In the NOAAM2 experiment the precipitation over land is almost the same as in CL91-00, despite the fact that the SSTs over sea are 1–1.5°C colder except for the coastal zone. This is especially the case in the first half of the month. This suggests that in particular the SSTs near the coast are important for the precipitation response over land. Under the prevailing dynamical conditions (see

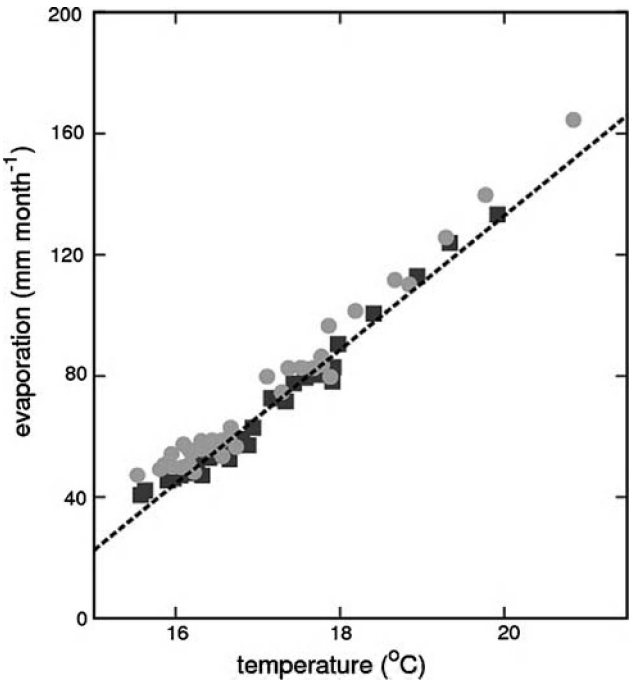


**Fig. 8** Relation between evaporation and SST. A *dot/square* denotes the average of a zone (as defined in Fig. 6). *Black squares* are averages over the month; *gray dots* are averages over the first 15 days of the month

Fig. 1) a strong hydrological cycle appears to be present with a large fraction of the enhanced evaporation precipitating in the coastal zone.

Extreme daily precipitation amounts are shown in Fig. 9. They are computed from the pool of data from the different stations (or grid boxes) in each zone (Fig. 6). For the 75th percentile, the observed and modeled precipitation amounts match well. However, for the more extreme 95th percentile the modeled precipitation amounts are too low. This may be related to the inability of RACMO2 to represent mesoscale organization of the convective complexes due to non-hydrostatic motions or to insufficient resolution to resolve the vigorous showers.

The coastal amplification compared to inland values (average of the 80–120 and 120–200 km zones) for the observations is shown in Fig. 10. Except for the most extreme 99th percentile, rainfall amounts in the coastal zone are approximately 30–40% higher than the inland values. For the most extreme events represented by the 99th percentiles the coastal amplification is smaller, between 10 and 20%. Partly, this may be due to statistical uncertainty. With on average 30–50 stations in a zone, the 99th percentile reflects only 9–15 events. Partly, it may also be explained by a longer lifetime of the strongest and largest convective complexes, which enables a further penetration inland.

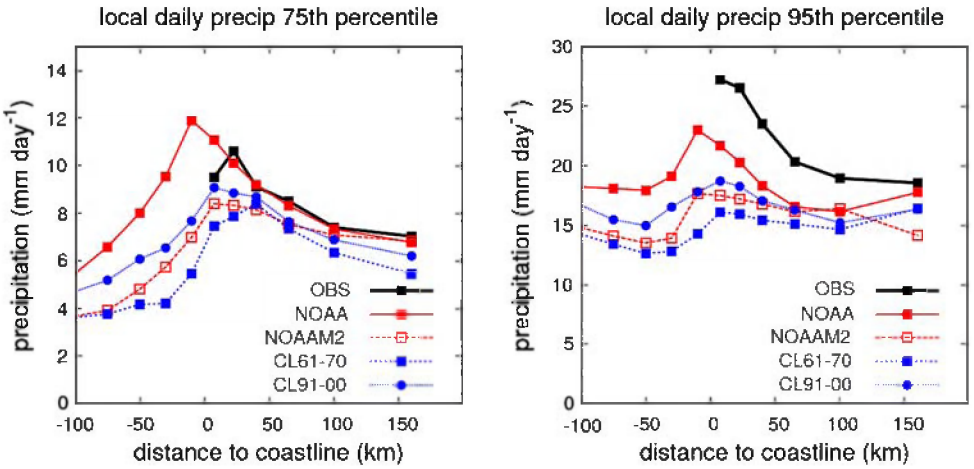


**Fig. 9** Extreme local (that is, station or *grid box*) daily precipitation amounts in August 2006 as a function of distance to the coast for the observations (*black solid*) and a selection of the model simulations (*colored lines*). Shown are the 75th (*left*) and 95th percentiles (*right*)

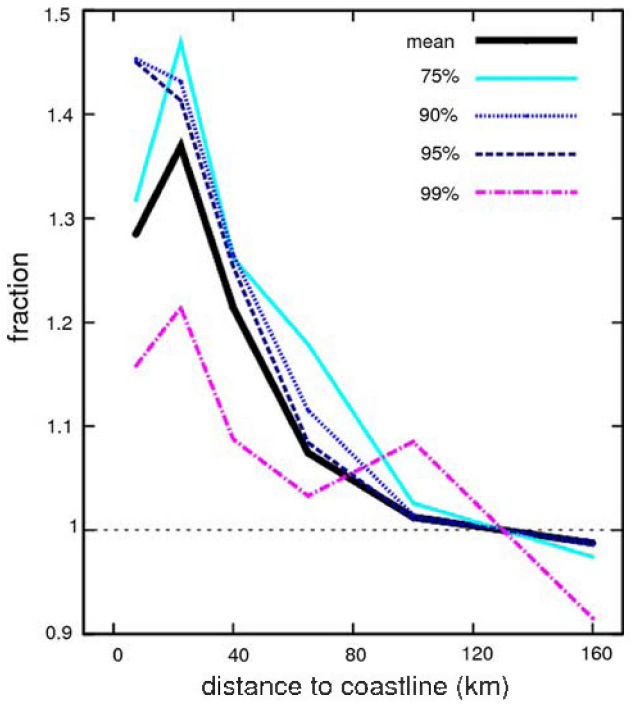


**Fig. 10** Observed mean and extreme precipitation amounts in August 2006 as a function of distance to the coast. Shown are relative differences (fraction) with respect to the observed average of the regions with distance of 80–120 and 120–200 km from the coastline

## 4 Relation between SST and precipitation derived from long-term observations

### 4.1 Data

The relation between SST and precipitation is analyzed in observational daily data for the period 1958–2006. The precipitation data, consisting of daily precipitation measurements at approximately 320 stations, is described in Sect. 2. As in Sect. 2, we use averages computed for the coastal region (less than 30 km from the coastline), the inland region (more than 30 km) and the total area of The Netherlands ("mean" in the plots). For the SST we used data from the ERA40 re-analysis (September 1957–August 2002) averaged over a relatively large box between 1 and 6°E, and 51.5 and 56°N. The period since September 2002 is supplemented by the operational ECMWF analysis. Although the temperature variations in the coastal zone are hardly resolved in this data set, it represents the most consistent and comprehensive long-term *daily* time series that is available. Time series measured at platforms or ships are typically only 10–20 years long or very inhomogeneous in time or in space. From the SST time series we computed the daily anomaly compared to the climatological mean. The climatological mean over the period 1958–2006 is computed for each month and then interpolated linearly in time in order to avoid stepwise discontinuities at the end of the month. Finally, to derive indices of the circulation we used ERA40 re-analysis data, again supplemented by the operational reanalysis for the last years.

### 4.2 Statistical model and results

On a monthly basis, it is difficult to find a causal relation between SSTs and precipitation. Physically, high SSTs cause higher evaporation rates and destabilize the atmosphere, and therefore enhance (coastal) precipitation—a positive correlation between SST and precipitation. This effect is clearly visible in the climatological mean precipitation in autumn when the sea is relatively warm compared to the land (see Fig. 2). However, there is also the possibility of an opposing, non-causal relation. Dry circulations tend to be warm (at least in summer) and cause (on a longer time scale) high SSTs, therefore giving rise to a negative correlation between SSTs and precipitation. So, high SSTs may result from a warm and dry circulation, but

may also occur with a cool and wet circulation and a warm history. A simple statistical analysis will not discriminate between these two cases. One may perform an analysis conditioned on the circulation type, but on a monthly mean basis the sample size is too small to obtain meaningful results.

Therefore, daily data is used to analyze the influence of the SSTs on precipitation. On a daily time scale the SST is primarily determined by the history, not by the circulation of that day. Because precipitation is mainly dependent on the circulation type, we first stratified the data according to the circulation. This is done by using the following statistical model:

$$P = c_w G_w + c_s G_s + c_v G_v + c_p M_p,$$

expressing the precipitation amount in terms of four components of the atmospheric circulation. These are the west component of the geostrophic wind ($G_w$), the south component ($G_s$), a measure of the vorticity ($G_v$) and the mean of the sea level pressure (MSLP or $M_p$). These measures are all computed from the sea level pressure within a relatively small domain between 49°–56°N and 0°–10°W (see Van Ulden and Van Oldenborgh 2006). The constants $c_w$, $c_s$, $c_v$, $c_p$ are computed by linear regression using the average daily precipitation computed from all precipitation stations in The Netherlands.

Given the regression coefficients, we compute the estimated precipitation amount $P_i$ for each day. We refer to $P_i$ as the precipitation circulation index or, shortly, circulation index. High (low) values of $P_i$ are mostly characterized by cyclonic west (anti cyclonic east) circulations.

For monthly means typically between 0.7 and 0.9 of the observed variance is explained with this method (Van Ulden and Van Oldenborgh 2006), but for daily precipitation amounts the explained variance is only 0.3–0.4. It is, however, not our purpose to build a statistical model to predict daily rainfall (in which case an explained variance of 0.4 would indeed imply a very low value), but to stratify (or bin) the data according to a circulation index. Because of the relatively small explained variance, we analyzed data of 3-month periods, thereby improving the signal-to-noise ratio compared to analyzing 1-month periods. Thus, August refers to the period July, August, September (JAS), and September to August, September, and October (ASO).

The binning of the data is done as follows. We divided the data in bins based on the value of $P_i$. The width of the bins is 1.8, which still gives a sufficient number of data (>100 days) for the bins with the more extreme wet circulations (high values of $P_i$). The exact choice of the lower (and upper) boundary value of each circulation bin turned out to have a moderately large influence on the results for the more extreme circulations (e.g., visible in the "jumpiness" of the dependencies for ASO in Fig. 13). We therefore took overlapping bins with steps of 0.6, so the first bin is 0–1.8, the second 0.6–2.4, and so forth. Thus, the data in the different bins are not independent. Bins containing less than 100 days are neglected, which effectively sets the stop criterion for the binning. In practice this depends on the time period analyzed. Figure 11 shows the average precipitation and the 10th, 25th, 50th, 75th and 90th percentiles for the data in each circulation bin. The average precipitation in the circulation bin closely follows the average circulation index $P_i$. The inter quartile range between the 25th and 75th percentiles (gray band in Fig. 11) shows that in each bin 50% of the data is reasonably close to the averaged precipitation in that bin. The "extreme" 90th percentile increases monotonically with $P_i$, except for $P_i > 6$, and thus $P_i$ also provides a useful circulation measure for the more extreme events. We note, however, that not all extremes occur with high values of $P_i$. On the one hand, the probability of an extreme precipitation event given the circulation index $P_i$ is smaller for low values of $P_i$, but on the other hand there are also more days with lower values of $P_i$. Of the days with precipitation amounts higher than the 95th percentile, typically 70% of the days have a $P_i > 4$ and 30% a $P_i > 6$.

For each circulation bin (defined by its $P_i$ values) the dependency of precipitation on the SST is estimated by a linear regression for the data (days) in the bin. This is done for both the coastal and the inland region. Within each bin the same days are used for both regions since the circulation index is only derived once for the average

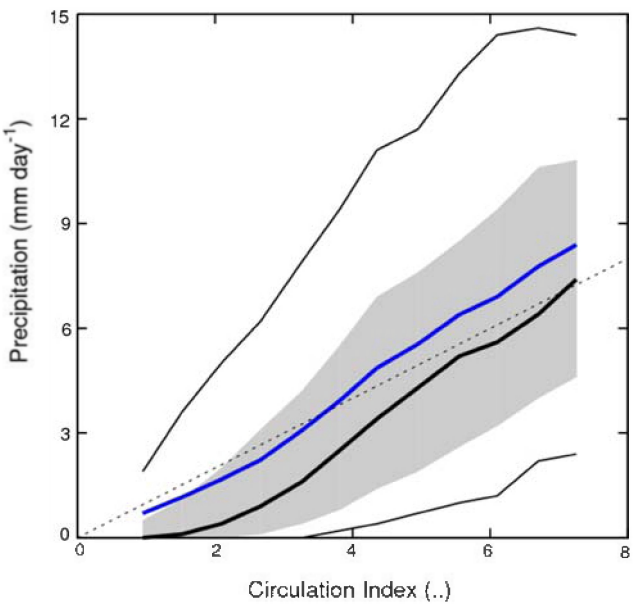


**Fig. 11** Mean precipitation in a circulation bin as a function of the average circulation index in the bin (*blue line*) for the period July, August, September (JAS). By construction it should be close to the 1–1 line (*dotted line*). The *gray band* denote the 25–75% range of the data, the *solid lines* the 10th, 50th, 90th percentiles

precipitation, and not separately for the regions. Therefore, the difference of the average precipitation in a bin between the coastal and the inland region provides a measure of the climatological difference between the coastal and inland region conditioned on the circulation.

As an example of the procedure, we show in Fig. 12 the daily precipitation amount in the coastal region versus the SST for two bins: one bin with a relatively dry circulation ($1.8 < P_i < 3.6$) and one bin with a wet circulation ($5.4 < P_i < 7.2$). Clearly, the scatter is large, with corresponding uncertainty in the fitted regression lines. Therefore, and in order to visualize the typical uncertainty, different fits to a number of subsets of the data are shown. It is reassuring that these different fits to different subsets of the data yield similar results. For the dry circulation there is a weak tendency for a negative dependency, but this dependency is not significant (90% level estimated by the bootstrap) in any of the fits. For the wet circulation bin, there is a statistically significant (90% level) positive dependency of the coastal precipitation between 11 and 15% per degree (approximately 1.5–2 times the CC relation). Taking 2006 (as an extreme year) out of the analysis results reduces the dependency from 15 to 12% per degree, but results with the data up to 1991 are again close to 15% per degree. Limiting the data to smaller SST anomalies or to smaller precipitation amounts again yields similar results. Finally, one may hypothesize that the found SST dependencies result from a correlation between SST and $P_i$, assuming that within a bin $P_i$ is a good measure for precipitation. The latter assumption is indeed realistic; we found a dependency of precipitation on $P_i$ in each bin rather close to the anticipated value of one (mostly between 0.7 and 1.4), which is surprisingly close considering that the bins contain only a small subset of the data from which $P_i$ was derived. Within a bin, however, there is no relation between the SST and $P_i$. To summarize, despite the fact that the signal-to-noise ratio is admittedly rather low, it turns out that there is a (direct) relation between SST and precipitation, which is reasonably robust.

Figure 13 shows for each bin the regression coefficients between precipitation and SST as a function of the average precipitation in that bin. Results of every third bin (containing independent data) are marked by a dot. We compare the regression coefficients with the values predicted by the CC relation (7% per degree). For each period considered there is a positive dependency of the precipitation on the SST in the more extreme circulation bins (with values of 5 and higher). The exception is late spring (April–May–June), when there is almost no dependency on the SST. In spring also the average precipitation in a circulation bin is smaller in the coastal zone than in the inland zone for the more extreme circulations, which reflects the climatological average state in spring, with lower precipitation amounts near the coast (see also Fig. 2). The dependency on SST increases strongly for the period midsummer and autumn. For the wet circulations (average precipitation amounts above 5 mm day$^{-1}$) dependencies are close to the CC relation for the inland region, and slightly higher than twice the CC relation for the coastal region. For the dryer circulation bins (precipitation below 4 mm day$^{-1}$) there is in general a negative dependency on the SST. In ASO (August, September, October) the relation between SST and precipitation is strongest with values approaching 2.5 times the CC relation for extreme events in the coastal area.

To highlight the causality of the relation between SST and precipitation, we divided the data in two halves based on the strength of the westerly wind. Naturally, a causal relation is primarily expected on days with westerly winds transporting moisture from sea to the land. We used the following criterion: westerly flows are defined by $G_w > 2$ m s$^{-1}$, and easterly flows by $G_w < 2$ m s$^{-1}$ (including some weak westerly flows in order to obtain sufficient days in this sub-

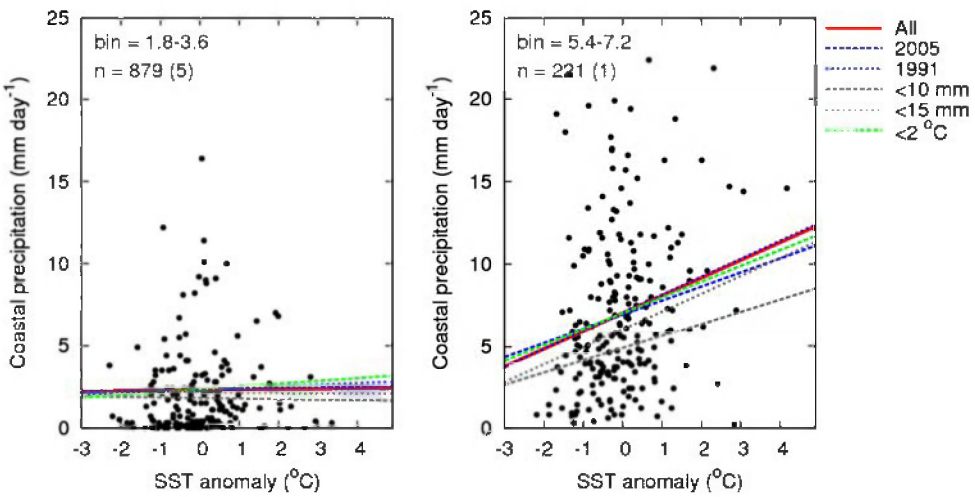


**Fig. 12** Coastal precipitation amounts versus the SST anomaly for two circulation bins (left relatively dry circulation, right wet circulation). Different fits to a number of selections of the data are shown; all: all days 1958–2006; 2005 (1991): all days from 1958 until 2005 (1991) (inclusive); <10 (15) mm: days with precipitation below 10 (15) mm day$^{-1}$; <2 K days with SST anomalies between −2 and +2 K

sample). The dependencies shown in Fig. 14 confirm the expected behavior. Days with westerly flows indeed have a positive dependency on the SST, which is stronger than the dependency obtained with all days. The remaining days on the other hand have no positive dependency on the SST; in fact, they even display a weak negative correlation. A plausible explanation might be that high SSTs can be linked to dry soils as both occur with a long history of warm and (presumably) dry days. Dry soil may act to reduce rainfall over land during episodes with prevailing easterly flows. Although we have not attempted to verify this hypothesis, the clear distinction between the dependencies for days with westerly flow and the remaining days confirm the causality of the relation between SST and precipitation.

Are the observations in August 2006 consistent with the statistical relations of Fig. 13? The circulation conditions in August were rather extreme. The average circulation index $P_i$ was 4.2, with 10 days above 5, and 4 days above 6. The average SST anomaly was 2.6°C, ranging between 1.7 and 4.2°C with the highest values during the first days of the month. Both contributed to the high precipitation amounts that were observed. To quantify this we reconstructed daily precipitation amounts using the daily values of $P_i$ and the SST anomaly combined with the statistical relationships as shown in Fig. 13. The circulation index provides the position on the $x$-axis in Fig. 13 for the different regions, which we will denote as the contribution of the circulation to the precipitation amount. In general this component is close to the circulation index $P_i$ itself. The circulation index also provides the SST dependency (on the $y$-axis in Fig. 13) and multiplied by the size of the SST anomaly it gives an estimate of the contribution of the SST anomaly to the precipitation amount. After summing up the daily contributions, the results are shown in Table 2. Using the statistical relations

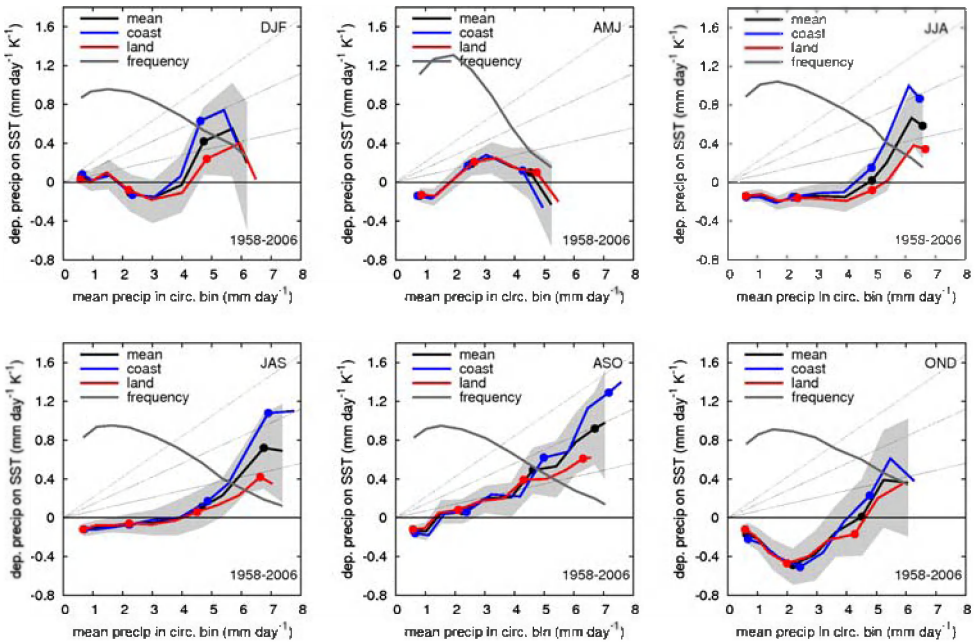


**Fig. 13** Regression coefficients of precipitation change (in mm day$^{-1}$ per degree SST) as a function of mean precipitation in each circulation bin. Results are plotted for the periods DJF, AMJ, JJA, JAS, ASO, OND, with particular emphasis on the late summer period. The *gray band* is the 10–90% uncertainty band in the estimation of the regression coefficient for the mean precipitation estimated by the bootstrap. Uncertainty bands for the coastal and inland zones are similar. The *thin lines* represent 1, 2, and 3 times the CC relation, respectively. The *thick gray line* is the number of days in each bin (divided by 1,500)

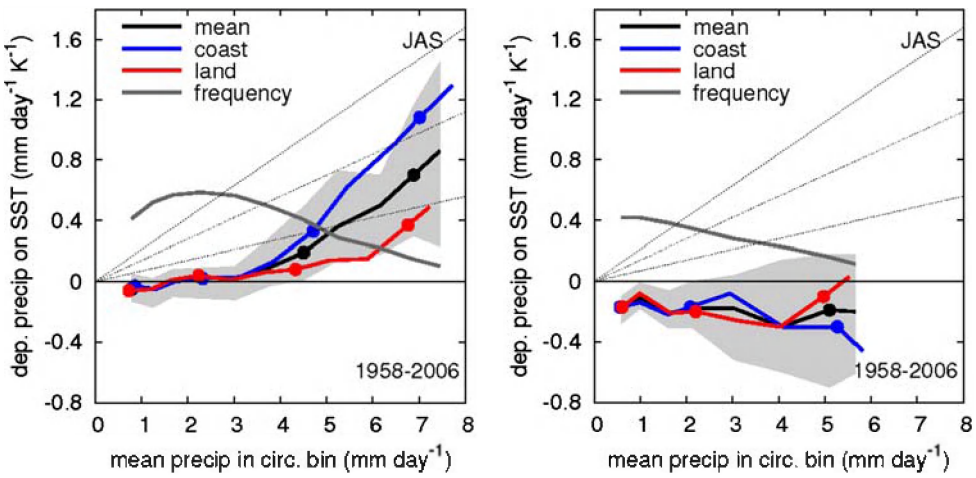


**Fig. 14** Same as Fig. 13, but now only for JAS, and separated in days with a westerly flow ($G_w > 2$ ms$^{-1}$) (*left panel*), and the remaining days ($G_w < 2$ ms$^{-1}$) (*right panel*)

**Table 2** Observed and reconstructed precipitation amounts for August 2006 using results of the statistical analysis

| | OBS | CIRC | SST | SUM |
|---|---|---|---|---|
| Coast | 210 | 132/137 | 26/44 | 158/181 |
| Land | 176 | 126/119 | 7/24 | 133/143 |
| Mean | 192 | 129/127 | 15/33 | 144/160 |

CIRC denotes the contribution of the circulation, SST the contribution of the sea surface temperature anomaly, and SUM the sum of both. The numbers before the "/" use results of the statistical analysis for JAS, the numbers after "/" use results for ASO

derived for JAS, the precipitation amounts are underestimated by about 40–50 mm month$^{-1}$ in all regions. The reconstructed precipitation yields a difference of 25 mm month$^{-1}$ (compared to the observed 34 mm month$^{-1}$) between the coastal and inland region, most of it related to the SST dependency. In relative terms, however, the difference between coastal and inland region is close to 17–18% in both observed and reconstructed precipitation. As a sensitivity experiment, the reconstructed precipitation is also computed using the relations derived for ASO. The absolute precipitation amounts are still underestimated by about 30 mm month$^{-1}$. The difference between the coastal and inland region increases to 38 mm month$^{-1}$ (24%).

Given that precipitation has a stochastic nature, and is obviously dependent on more factors than $P_i$ and SST only, we think that the agreement between the constructed and observed precipitation is fair. For example, the RACMO results suggest that small details in the SST in the coastal zone have a significant impact on precipitation amounts in the coastal zone. This effect is (due to a lack of observations) not captured in the coarse resolution SST time series used in the statistical analysis.

Finally, we would like to emphasize that, although the statistical dependency of precipitation on SST appears to be robust, the uncertainty is also relatively large. The uncertainty is illustrated by the gray bands in Fig. 13 and by the different fits to subsets of the data in Fig. 12. Still, for late summer (JJA, JAS, ASO) all results of the different subsets of the data (e.g., different time periods; not all shown) have in common that for the wettest circulation ($P_i \geq 6$) the regression coefficient approaches approximately 1.5–2.5 times the CC relation for the coastal zone, and approximately 0–1 times the CC relation for the inland zone.

## 5 Discussion

### 5.1 Relation to the Clausius–Clapeyron relation

In the literature two physical constraints are commonly mentioned in relation to precipitation changes due to climate change. On a global scale mean precipitation in GCMs increases at a rate of 1–3% per degree. This behavior appears well understood from energy budget considerations; one percent increase in precipitation equals approximately 1 W m$^{-2}$, which is a significant term in comparison with greenhouse gas forcing (Allen and Ingram 2002). The other constraint is the CC relation, which determines the water vapor content of the atmosphere in saturated conditions. GCM model evidence indicates that the CC relation is a good indicator for changes in the extremes (Pall et al. 2007). On the scale of showers (not resolved by the GCMs) the CC relation may be exceeded because the latent heat release feeds back on the cloud dynamics, and therefore on the atmospheric moisture convergence. However, the extent to which the CC relation can be exceeded is limited by the amount of water available in the atmosphere: if the shower intensity is high it will dry out the environment, which will suppress the intensity. In this paper we nevertheless find stronger dependencies in the order of 1.5–2.5 times the CC relation. Where does the moisture come from? The regional model results clearly indicate that a large part of the additional moisture comes from enhanced evaporation above sea. Figure 8 shows a dependency of evaporation on the SST of approximately three times the CC relation. Although we realize that the modeling results of the case study do not necessarily apply in general, it appears a reasonable hypothesis that (local) surface evaporation above sea provides a considerable source of additional moisture for the coastal areas (see also Persson et al. 2005; Lebeaupin et al. 2006).

### 5.2 Relation to climate change scenarios and regional climate modeling studies

Recently, a set of four climate scenarios was issued for the Netherlands (Lenderink et al. 2007; van den Hurk et al. 2006). These scenarios were based on combined information from global and regional modeling studies. The regional modeling results were from PRUDENCE, an EU funded project which ran from 2001 to 2004 (Christensen et al. 2007a). With the present results in mind there are two points that are worth noting. First, the RCMs have been operated at a relatively coarse resolution of 50 km, which at that time was state-of-the-art. Clearly, this resolution is not sufficient to resolve the coastal effects found in this paper. Results with RACMO2 (not shown) indicate that we start to resolve coastal effects at a resolution of 25 km. At a 12 km resolution the results strongly resemble the results obtained at 6 km resolution. Second, none of the models have operated a model of the North Sea (one of the RCMs, RCAO, included a model for the Baltic sea). Instead, SSTs

were prescribed from the global model. The global models do not resolve the North Sea well, and it is likely that the temperature changes are biased towards those in the Atlantic Ocean. In many GCM simulations, as in the HadAM3H simulation used in PRUDENCE, Atlantic SSTs rise much slower than the global mean temperature (Van Ulden and Van Oldenborgh 2006).

Even at higher resolutions RACMO2 still underestimates precipitation extremes on the local scale. The model seems to have problems with simulating the organization of mesoscale convective systems, which were frequently observed during August 2006 and which produced very high local rainfall amounts. In addition, too much precipitation falls over sea and not enough over land. This could well be related to the fact that most convective parameterizations are diagnostic; they react (almost) instantaneous to changes in the atmospheric stability and do not simulate a realistic convective cloud development (Guichard et al. 2004). Non-hydrostatic modeling, in which case convective clouds are resolved rather than parameterized, may be needed to improve these aspects. This hypothesis has not been tested, but we think that August 2006 could be a very interesting period to evaluate non-hydrostatic models.

Can we expect more events like August 2006 in the future climate? Of course, the answer strongly depends on the atmospheric circulation. In particular, it depends on how often a similar sequence of a very warm circulation followed by a rapid transition to a cold anti-cyclonic circulation will occur in the future climate. At the moment, this is difficult to assess from GCMs. Preferably ensembles of GCM integrations are needed to separate the natural variability from the climate change signal. In addition, GCMs should be better evaluated, and improved, with respect to their ability to simulate transitions between the atmospheric circulation regimes. However, given that the frequency of these events does not change, it is likely that the rise in SSTs will cause an increase in coastal rainfall, as supported by the trends in precipitation over the last 55 years. Since the North Sea is shallow it is also likely that it will more closely follow the larger temperature rise above the continent compared to the (Atlantic) ocean. Thus, the local temperature rise in the North Sea may be considerably larger than the temperature rise in the Atlantic Ocean, giving rise to stronger coastal changes in precipitation.

## 6 Conclusions

The impact of coastal SSTs of the North Sea on summertime precipitation in The Netherlands is analyzed with RCM integrations for August 2006 and with observations from the period 1958–2006.

August 2006 was characterized by a cold and wet Northwesterly circulation, which—in combination with high SSTs inherited from a very warm July—brought excessive precipitation amounts in the Netherlands, in particular in areas close to the sea. With the regional climate model RACMO2 hindcast simulations for August 2006 have been performed. The regional model reproduces the overall rainfall structure with the highest amounts close to the sea when using the observed SSTs (reference run). On a more detailed level, however, the model fails to reproduce the exact spatial distribution (too much rain too close to the coast) and tends to underestimate the strongest daily events. In a set of sensitivity experiments the dependency of precipitation on the SST is investigated. In experiments with a 2° lower SST compared to the reference, coastal rainfall amounts are approximately 30% lower, yielding a temperature dependency close to two times the CC relation.

The relation between SST, atmospheric circulation, and precipitation is further analyzed statistically on the basis of daily observations in the period 1958–2006. Under favorable circulation conditions—mostly cyclonic westerly flows—dependencies of coastal precipitation on the SST again amount to approximately two times the CC relation. These relations are consistent with the observed precipitation amounts during August 2006. The trend in mean precipitation (1951–2006) in summer shows that the coastal zone is progressively getting wetter compared to the inland zone. At the same time, it is found that the SSTs have risen approximately two times faster than the global mean temperature. The positive trend in the difference between coastal and inland precipitation seems to be a robust finding as it is quite insensitive to the precise choice of the period of analysis. In contrast, the trend in precipitation itself is highly dependent on the analyzed period for both regions.

In summary, the results show a strong influence of near-coastal SSTs on precipitation in the coastal areas of the Netherlands on all timescales—dependencies that may significantly exceed the CC relation. Although the situation may be rather specific for the Netherlands, we are convinced that the results have a wider implication and that high resolution modeling, including realistic representations of coastal seas, is needed to provide climate change scenarios for coastal areas.

**Acknowledgments** We thank Hans Roozekrans for providing the NAOO satellite measurements, and Rudmer Jilderda (KNMI Climate Services Department) for the precipitation measurements. We thank Albert Klein Tank, Aad van Ulden and Bart van den Hurk for valuable comments on this work. This work has been supported by the Dutch Climate Change and Spatial Planning program (BSIK) and by the European FP-6 project ENSEMBLES (GOCE-CT-2003-505539).

## References


Allen MR, Ingram WJ (2002) Constraints on the future changes in climate and the hydrological cycle. Nature 419:224–232

Benestad RE, Melsom A (2002) Is there a link between unusually wet autumns in southeastern Norway and sea-surface temperature anomalies? Clim Res 23:67–79

Christensen JH, Christensen OB (2003) Climate modelling: severe summertime flooding in Europe. Nature 421:805–806

Christensen JH, Carter TR, Rummukainen M, Amanatidis G (2007a) Evaluating the performance and utility of regional climate models: the PRUDENCE project. Clim Change 81:1–6. doi:10.1007/s10584-006-9211-6

Christensen JH, Hewitson B, Busuioc A, Chen A, Gao X, Held I, Jones R, Kolli RK, Kwon W-T, Laprise R, Magaña Rueda V, Mearns L, Menéndez CG, Räisänen J, Rinke A, Sarr A, Whetton P (2007b) Regional climate projections. In: Solomon S, Qin D, Manning M, Chen Z, Marquis M, Averyt KB, Tignor M, Miller HL (eds) Climate change 2007: the physical science basis. Contribution of Working Group I to the fourth assessment report of the Intergovernmental Panel on Climate Change. Cambridge University Press, Cambridge

Frei C, Schöll R, Fukutome S, Schmidli J, Vidale PL (2006) Future change of precipitation extremes in Europe: intercomparison of scenarios from regional climate models. J Geophys Res 111:D06105. doi:10.1029/2005JD005965

Groisman PYa, Knight RW, Easterling DR, Karl TR, Hegerl GC, Razuvaev VN (2005) Trends in intense precipitation in the climate record. J Clim 18:1326–1350

Guichard F, Petch JC, Redelsperger J-L, Bechtold P, Chaboureau J-P, Cheinet S, Grabowski W, Grenier H, Jones CG, Köhler M, Piriou J-M, Tailleux R, Tomasini M (2004) Modelling the diurnal cycle of deep precipitating convection over land with cloud-resolving models and single-column models. Q J Roy Meteor Soc 130:3139–3172

Held IM, Soden BJ (2006) Robust responses of the hydrological cycle to global warming. J Clim 19:5686–5699

Hewitt CD, Griggs DJ (2004) Ensembles-based predictions of climate changes and their impacts (ENSEMBLES). EOS 85:566

Van den Hurk BJJM, Klein Tank AMG, Lenderink G, Van Ulden AP, Van Oldenborgh GJ, Katsman CA, Van den Brink HW, Keller F, Bessembinder JJF, Burgers G, Komen GJ, Hazeleger W, Drijfhout SS (2006) KNMI Climate Change Scenarios 2006 for the Netherlands. KNMI-publication WR-2006-01, pp 82. Available at http://www.knmi.nl/climatescenarios/

Kjellström E, Ruosteenoja K (2007) Present-day and future precipitation in the Baltic Sea region as simulated in a suite of regional climate models. Clim Change 81:281–291. doi:10.1007/s10584-006-9219-y

Kjellström E, Döscher R, Markus Meier HE (2005) Atmospheric response to different sea surface temperatures in the Baltic Sea: coupled versus uncoupled regional climate model experiments. Nord Hydrol 36:397–409

Lebeaupin C, Ducrocq V, Giordani H (2006) Sensitivity of torrential rain events to the sea surface temperature based on high-resolution numerical forecasts. J Geophys Res 111:D12110. doi:10.1029/2005JD006541

Lenderink G, Van den Hurk B, Van Meijgaard E, Van Ulden A, Cuijpers H (2003) Simulation of present-day climate in RACMO2: first results and model developments. KNMI technical report, TR-252

Lenderink G, Van Ulden A, Van den Hurk B, Keller F (2007) A study on combining global and regional climate model results for generating climate scenarios of temperature and precipitation for the Netherlands. Clim Dyn. doi:10.1007/s00382-008-0366-x

Messager C, Gallée, Brasseur O (2004) Precipitation sensitivity to regional SST in a regional climate in a regional climate simulation during the West African monsoon for two dry years. Clim Dyn 22:249–266. doi:10.1007/s00382-003-0381-x

Pall P, Allen MR, Stone DA (2007) Testing the Clausius–Capeyron constraint on changes in extreme precipitation under $CO_2$ warming. Clim Dyn 28:351–363. doi:10.1007/s00382-006-0180-2

Persson POG, Neiman PJ, Walter B, Bao J-W, Ralph FM (2005) Contributions from California coastal-zone surface fluxes to heavy coastal precipitation: a CALJET Case Study during the strong El Niño of 1998. Mon Weather Rev 133:1175–1198

Räisänen J, Hansson U, Ullerstig A, Döscher R, Graham L, Jones C, Meier H, Samuelsson P, Willén U (2004) European climate in the late twenty-first century: regional simulations with two driving global models and two forcing secnarios. Clim Dyn 22:13–31. doi:10.1007/s00382-003-0365-x

Rayner NA, Brohan P, Parker DE, Folland CK, Kennedy JJ, Vanicek M, Ansell T, Tett SFB (2006) Improved analyses of changes and uncertainties in sea surface temperature measured in situ since the mid-nineteenth century: the HadSST2 data set. J Clim 19(3):446–469

Rowell DP (2003) The impact of Mediterranean SSTs on the Sahelian rainfall season. J Clim 16:849–862

Semmler T, Jacob D (2004) Modeling extreme precipitation events—a climate change simulation for Europe. Glob Planet Change 44:119–127

Seneviratne SI, Pal JS, Eltahir EAB, Schär C (2002) Summer dryness in a warmer climate: a process study with a regional climate model. Clim Dyn 20:69–85

Somot S, Sevault F, Déqué M, Crépon M (2007) 21st Century climate change scenario for the Mediterranean using a coupled atmosphere–ocean regional climate model. Glob Planet Change. doi:10.1016/j.gloplacha.2007.10.003

Trenberth KE, Dai A, Rasmussen RM, Parsons DB (2003) The changing character of precipitation. Bull Am Meteor Soc 1205–1217

Uppala SM, 45 co-autors (2005) The ERA-40 re-analysis. Q J Roy Meteorol Soc 131:2961–3012. doi:10.1256/qj.04.176

Van Ulden AP, Van Oldenborgh GJ (2006) Large-scale atmospheric circulation biases in global climate model simulations and their importance for climate change in Central Europe. Atmos Chem Phys 6:863–881

Vidale PL, Lüthi D, Wegmann R, Schär C (2007) European summer climate variability in a heterogeneous multi-model ensemble. Clim Change 81:209–232

Webster PJ, Holland GJ, Curry JA, Chang H-R (2005) Changes in tropical cyclone number, duration, and intensity in a warming environment. 309:1844–1846

Yin JH (2005) A consistent poleward shift of the storm tracks in simulations of 21st century climate. Geophys Res Lett 32:L18701. doi:10.1029/2005GL023684